



Theses and Dissertations

2009-12-14

Energy Dissipation Caused by Asphalt Roadway Gouges for Use in Accident Reconstruction

Charles L. Crosby
Brigham Young University - Provo

Follow this and additional works at: <https://scholarsarchive.byu.edu/etd>



Part of the [Mechanical Engineering Commons](#)

BYU ScholarsArchive Citation

Crosby, Charles L., "Energy Dissipation Caused by Asphalt Roadway Gouges for Use in Accident Reconstruction" (2009). *Theses and Dissertations*. 1983.
<https://scholarsarchive.byu.edu/etd/1983>

This Thesis is brought to you for free and open access by BYU ScholarsArchive. It has been accepted for inclusion in Theses and Dissertations by an authorized administrator of BYU ScholarsArchive. For more information, please contact scholarsarchive@byu.edu, ellen_amatangelo@byu.edu.

Energy Dissipation Caused by Asphalt Roadway Gouges
For Use in Accident Reconstruction

Charles L. Crosby

A thesis submitted to the faculty of
Brigham Young University
in partial fulfillment of the requirements for the degree of
Master of Science

Kenneth W. Chase, Chair
Mark B. Colton
Brian D. Jensen

Department of Mechanical Engineering
Brigham Young University

April 2010

Copyright © 2010 Charles L. Crosby

All Rights Reserved

ABSTRACT

Energy Dissipation Caused by Asphalt Roadway Gouges

For Use in Accident Reconstruction

Charles L. Crosby

Department of Mechanical Engineering

Master of Science

In reconstruction of on-roadway vehicle accidents, roadway surface gouges and the forces and energy attributed to the related vehicle components become important keys to resolving an accurate accident reconstruction. These roadway gouge forces vary depending upon such factors as surface temperature and the velocity and geometry of the gouging mechanism. Accounting for the forces applied to vehicle components and the energy dissipated from such forces can be helpful in accident reconstruction where supporting data exists.

This research documents the force necessary to create a given roadway gouge geometry. Controlled pavement gouging tests were performed using roadway surface temperature and gouging velocity as main factors. The results of this testing and analysis are useful in quantifying gouge forces and energies for use in accident reconstruction. The findings show that the temperature of the roadway surface that is being damaged significantly affects the amount of force required to cause the damage. A summary of experiments and techniques as applied to accident reconstruction are presented.

Keywords: accident reconstruction, pavement, gouge, road, damage, force, energy

ACKNOWLEDGMENTS

I would like to thank all of the engineers and employees at Collision Safety Engineering, LLC. for their continued support of my journey in academics and for encouraging me to continue my education. I would especially like to thank Mark Warner who I have had the pleasure of co-authoring many technical publications with and who was a big supporter and participant in the research presented in this paper. Without his help and ideas, this publication would not have happened.

I would also like to thank the many professors and faculty members at Brigham Young University. Your help and encouragement really influenced my learning and education throughout my undergraduate and graduate career there.

Most of all, I am extremely grateful to my loving wife for her continued support and encouragement. She never doubted that I would be able to complete my schooling and did everything she could to make sure it actually happened. Her love, patience, and determination were examples in my life and were the reason I am the person I am today. Thank you!

TABLE OF CONTENTS

LIST OF TABLES	vii
LIST OF FIGURES	ix
1 Introduction.....	1
2 Background	3
2.1 Statistics and Uses of Accident Reconstruction	3
2.2 Accident Reconstruction Methods.....	3
2.2.1 Motion Analysis.....	4
2.2.2 Avoidance Analysis	4
2.2.3 Collision Analysis.....	5
2.2.4 Force Analysis	5
2.3 Force and Energy in Accident Reconstruction	6
2.4 Roadway Gouge Energy Calculation.....	8
2.5 Roadway Surfaces.....	12
2.5.1 Rigid Pavements	12
2.5.2 Cold Mix Asphalt Pavements	13
2.5.3 Chip Seal Roadway Surfaces	14
2.5.4 Hot Mix Asphalt	15
3 Test Method.....	17
3.1 Test Vehicle Set-up.....	17
3.2 Test Conditions – Vehicle.....	20
3.3 Test Conditions – Roadway	21
3.4 Test Procedure	22
3.5 Measurement Method	23

3.6	Accelerometer Data	26
4	Results	31
5	Conclusions	39
5.1	Test Method	39
5.2	Test Results.....	39
5.3	Reconstruction Implication.....	40
6	Future Research	41
	References.....	43
	Appendix A Raw Test data	47
	Appendix B Photographs	51

LIST OF TABLES

Table 3.1 Summary of Test Conditions for Each Test.....	22
Table 4.1 Summary of Tests Performed	36
Table 5.1 Summary of Test Results	39
Table A.1 Raw Test Data of 15mph Test at 95° F.....	47
Table A.2 Cross-section Area and Force of 15mph Test at 95° F.....	49

LIST OF FIGURES

Figure 2.1	Example of a roadway gouge caused by a rolling vehicle	9
Figure 2.2	Example of a roadway gouge caused by a wheel rim	10
Figure 2.3	Test vehicle setup of previous testing done [Warner 2008]	11
Figure 2.4	Example of a concrete roadway surface [FHWA]	13
Figure 2.5	Example of cold mix asphalt patching [Layfayette].....	14
Figure 2.6	Example of newly paved chip seal [San Juan County News]	15
Figure 2.7	Example of HMA roadway surface	16
Figure 3.1	Picture of gouge tooth used during testing	18
Figure 3.2	Gouge test vehicle configuration.....	19
Figure 3.3	Tape measure next to gouge	24
Figure 3.4	Contour gage used for profile measurements	25
Figure 3.5	Example of photograph used to record gouge profile	25
Figure 3.6	CAD drawing of gouge profile used for area measurement.....	26
Figure 3.7	Example of raw accelerometer data vs. corrected accelerometer data	28
Figure 4.1	Post-test roadway gouge.....	31
Figure 4.2	Asphalt gouge at 15 mph at 95° F surface temperature	32
Figure 4.3	Asphalt gouge at 15 mph at 95° F showing all points.....	33
Figure 4.4	Asphalt gouge at 15 mph at 133° F	35
Figure 4.5	Asphalt gouge at 25 mph at 104° F	36
Figure 4.6	Pressure v. temperature of the tests completed	37
Figure 4.7	Modulus of asphalt	38

1 INTRODUCTION

Roadway gouges are common during impact and rollover crashes, and can be helpful in analysis of vehicle motion and energy dissipation during many phases of a crash. A variety of different techniques in accident reconstruction are used today to determine crash characteristics, such as vehicle speed and direction, override/underride relationships, yaw rate, roll rate, etc. Most of these techniques are highly dependent on knowing or estimating the total energy involved in the crash [Brach] and use physics to resolve these energies into forces, velocities, accelerations, and distances. Different aspects of vehicle crashes use unique data sets to obtain estimates of individual crash energies which can then be combined to form a total reconstruction. For example, barrier crash tests provide a good basis for measuring crush energy on the front [Campbell, Neptune 1994, Warner C], the rear [Croteau] or even the side [Neptune 1998, Strother 1998, Warner M 2004] of an impacted vehicle. Tire marks can be used to determine pre-impact or pre-rollover energies of a skidding vehicle [Varat, Wallingford]. Rollover testing provides information that can be used to estimate force and energy parameters during the rollover phase of an accident [Orlowski]. However, little research has been done to quantify the forces and energy associated with roadway gouges or similar roadway damage patterns. A number of authors doing other studies in the field of accident reconstruction have mentioned the need and benefit of such information [Marine]. Availability of such information would fill the gap in several aspects of accident reconstruction. For example, in a rollover crash, a large gouge in the roadway due to the rolling vehicle can be correlated to forces applied to vehicle

components and may aid in calculating vehicle translation, roll rate, occupant motion, etc. A small amount of research has been done in the area to quantify the amount of force and energy that a roadway gouge absorbed under controlled test conditions [Warner M 2008]. Those results are compared to the results obtained by this research. The current testing also presents gouges at higher speeds than previously conducted as well as a larger temperature variation and thus provides a greater range of gouge energies to analyze.

2 BACKGROUND

2.1 Statistics and Uses of Accident Reconstruction

In 2008, nearly six million police-reported motor vehicle crashes occurred. About 40% of those accidents involved injuries and over 37,000 resulted in fatalities [NHTSA]. Accident reconstruction techniques are applied to many of these crashes for a wide variety of reasons. Car manufacturers can use the information obtained from a detailed accident reconstruction to determine what, if anything, went wrong during a particular crash. That knowledge can then be used to further improve the design and safety of future vehicles or determine if recalls are necessary on existing vehicles. Law enforcement personnel use accident reconstruction to determine at-fault individuals and to assess whether criminal charges need to be filed. Insurance companies use the information to determine what payouts may need to be made in collisions involving their clients. Lawyers use the accident reconstruction as their basis for civil litigation, both on the plaintiff's side as well as the defense. The more detailed the information that is found in accident reconstruction, the easier conclusions can be made about the accident and a greater certainty about those conclusions can be obtained.

2.2 Accident Reconstruction Methods

There are several methods used in the process of vehicular accident reconstruction. Some of these are more useful in certain situations than others and many of the methods can be used

together to reconstruct parts of a crash. These parts can later be combined to get an overall reconstruction. In 1978, a book was published by Rudolf Limpert [Limpert] that outlined his ideas of the different methods that could be used to analyze a crash. Since then others have shared their ideas as well [Baker, Brach, Fricke, Gillespie]. While everyone has different names for the methods and breaks the methods down into different groups, all seem to have the same or similar four general methods: motion analysis, avoidance analysis, collision analysis, and force analysis. Examples are given in the texts on how to apply each of these techniques to obtain a full reconstruction of the accident. Over the years, these methods have been refined because of the continuation of research and testing.

2.2.1 Motion Analysis

Motion analysis started out as simple physics equations to simulate the crash and estimate the forces and motion. While the basic equations still remain the foundation of this method, computer programs that are able to do enormous amounts of calculations quickly [PC Crash, SMAC] have become the norm. These programs have broadened the amount of data and family of inputs that can be used to calculate motion.

2.2.2 Avoidance Analysis

Avoidance analysis is used to study the tendencies and reactions of the drivers of motor vehicles. This includes things such as driver reaction time, driver tendencies, alcohol effects, driver distraction effects (like talking or texting on a cellular phone), and field of view [Sens, Uchida, Vilardo]. Many of these aspects have been studied in great detail over the years and have evolved to become very well known and somewhat standardized. When some of the earlier

books and papers were written, the authors couldn't have imagined that cellular phone use would be an important part of the accident reconstruction process.

2.2.3 Collision Analysis

Collision analysis attempts to quantify forces and energies associated with deformation of vehicle structures during collisions. This method of accident reconstruction is in many ways the basis of any crash involving significant vehicle damage. When a vehicle is involved in a crash where measurable damage occurred, equations can be applied to determine the amount of crush energy the vehicle absorbed. Measurements of the crush are taken and compared to controlled crash tests to calculate the crush energy. This energy can then be used to determine collision factors such as pre-impact speed, post-impact speed, decelerations, etc. The energy that is absorbed by a crushing vehicle is typically the largest source of energy dissipation in most motor vehicle collisions. Because of this, it has received a large amount of interest from the accident reconstruction community and has a large body of research and testing as supporting material. Over the years, this method has had increasing amounts of data and many individuals working on refining this type of analysis [Campbell, Croteau, Neptune 1994, Neptune 1998, Strother 1986, Strother 1998, Warner C, Warner M].

2.2.4 Force Analysis

Force analysis is typically used to determine and quantify any and all forces acting on a vehicle before and after a collision. A common example is tire friction. The interaction between the tire and the roadway has been studied over the years in great detail [Baker, Fricke, Gillespie, Wallingford]. Other forces are calculated or estimated as well. These include forces due to engine load, aerodynamic drag, average friction over a given distance due to a rolling vehicle,

etc. However, the forces created due to roadway damage have yet to be sufficiently researched and quantified. This lack of data is the gap in the force analysis method of accident reconstruction that the current research is attempting to fill. Quantifying the gouge force will provide yet another tool to assist in the accident reconstruction process.

2.3 Force and Energy in Accident Reconstruction

The principle behind using forces and energies in accident reconstruction is the law of conservation of energy. This law states that energy can be neither created nor destroyed, but can only be converted from one form to another. The best way to explain how this pertains to accident reconstruction is a simple example with supporting equations. A vehicle traveling at a given velocity has a kinetic energy that can be expressed by

$$KE = \frac{1}{2}mv^2 = \frac{1}{2}\frac{w}{g}v^2 \quad (2.1)$$

Where m = mass and w = weight of the vehicle, g = acceleration due to gravity, and v = velocity. This is the total energy that a vehicle possesses prior to a crash. During the crash, the energy is absorbed and dissipated in possibly many different ways. Before or after an impact, a driver may apply brakes, which could cause the car to skid. The friction force exerted on the vehicle due to the tire-roadway interaction can be used to calculate energy dissipation. The calculated energy of a skidding tire has been studied and addressed in testing and research [Wallingford] and has been well documented in books and other publications [Gillespie]. A vehicle that collides with another vehicle or object will lose energy while it is being crushed and deformed. This energy is called the crush energy of a vehicle. There are different methods for estimating the crush energy of a vehicle and each has its associated testing and research to validate the methods. These methods

will not be discussed in depth here but can be found in other publications [Campbell, Croteau, Neptune 1994, Neptune 1998, Strother 1986, Strother 1998, Warner C, Warner M].

Other energies that may be of interest depending on the circumstances of the crash in question could be yaw energy (the energy of a rotating object), roll energy (the energy of a rolling object), the change in potential energy based on slope or elevation change, and roadway gouge energy. All of these energies or a combination of these energies is the basis for performing an accident reconstruction using force and energy methods. This is done by adding up all of the energies and equating them to the total initial energy (KE_i) before any skidding, colliding, or maneuvering has occurred as shown by

$$KE_i = KE_{trans} + KE_{yaw} + KE_{roll} + CE + E_f + E_{gouge} + \Delta PE \quad (2.2)$$

Where the energies involved are

$$KE_i = \text{Initial translational energy} = KE_i = \frac{1}{2}mv_i^2 \quad (2.3)$$

$$KE_{trans} = \text{Dissipated translational energy} = KE_{trans} = \frac{1}{2}mv_{trans}^2 \quad (2.4)$$

$$KE_{yaw} = \text{Yaw energy} = KE_{yaw} = \frac{1}{2}I_{yaw}\Omega_{yaw}^2 \quad (2.5)$$

$$KE_{roll} = \text{Roll energy} = KE_{roll} = \frac{1}{2}I_{roll}\Omega_{roll}^2 \quad (2.6)$$

CE = Crush Energy

$$E_f = \text{Tire friction energy} = E_f = \mu Nd \quad (2.7)$$

E_{gouge} = Gouge energy

$$\Delta PE = \text{Change in gravitational potential energy} = \Delta PE = mg\Delta h \quad (2.8)$$

And the vehicle parameters include:

m = mass of the vehicle

v_i = initial velocity of the vehicle

I_{yaw} = yaw moment of inertia

Ω_{yaw} = yaw rotation rate

I_{roll} = roll moment of inertia

Ω_{roll} = roll rotation rate

μ = coefficient of friction

N = normal force

d = distance of tire mark

g = acceleration due to gravity

h = height of the center of gravity

It is the job of the individual who is investigating a crash to estimate realistic values for each of these numbers and equations. The goal is typically to solve the equations to determine initial velocity (v_i). However, other unknowns may be solved for depending on what values are initially known or can reasonably be estimated. Until recently, the value of gouge energy had to be estimated merely based on the experience and intuition of the individual performing the reconstruction of a crash. Little research or testing had been performed to form the basis of any such calculation.

2.4 Roadway Gouge Energy Calculation

Roadway gouging is a common occurrence in on-road motor vehicle collisions. Nearly all on-road rollover accidents leave some sort of roadway damage due to the interaction of hard, stiff body members with the roadway surface. Vehicle collisions where one or more vehicles lose tire pressure, or lose an entire wheel, also expose stiff vehicle members to the roadway. These

can be wheel rims, A-arms, shocks, and other suspension members as well as underside body parts. The gouges caused by such interaction can take drastically different shapes from narrow to wide, from shallow to very deep. Figure 2.1 and Figure 2.2 show examples of roadway gouges caused by a rolling vehicle and the rim of a vehicle moving along the roadway surface.

In an accident reconstruction book published in 2005, the authors stated, “An accurate reconstruction cannot be carried out without a good investigation” [Brach]. This includes measuring and documenting any and all gouges caused during the vehicle collision. These measurements can then be compared to control testing that has been performed to quantify the



Figure 2.1 Example of a roadway gouge caused by a rolling vehicle



Figure 2.2 Example of a roadway gouge caused by a wheel rim

results of the data taken. In 2008, the first and only testing performed on the subject of roadway gouging showed some basic results [Warner M]. The testing done was performed at slow speed (7 mph). A gouge was created using a one inch “tooth” which was a one inch diameter grade 8 bolt. The test vehicle (a Compact Moving Barrier or CMB) was brought up to speed using a pendulum effect. Figure 2.3 shows a drawing on how the test vehicle was deployed. Once the test vehicle was released from height, the potential energy was converted to kinetic energy. When it reached the roadway, the vehicle was released from any connecting forces and allowed to move freely with only the gouge creating the force required to slow the vehicle down.

The gouge’s length and depth were then measured and from this measurement, a pressure (force per square inch) was calculated. No accelerometer was used and thus only average forces and pressure could be calculated along the entire length of the gouge. The testing found an average pressure of 5223 psi over the length of the gouge. This finding was the first actual

number that allowed an individual to make an energy estimation of a gouge based on testing and not based on an assumption. To make the estimate, the gouge in question must be measured, both length and depth. The average cross-sectional area is calculated. This number is then multiplied by the average pressure to get a force. That force can then be multiplied by the total length of the

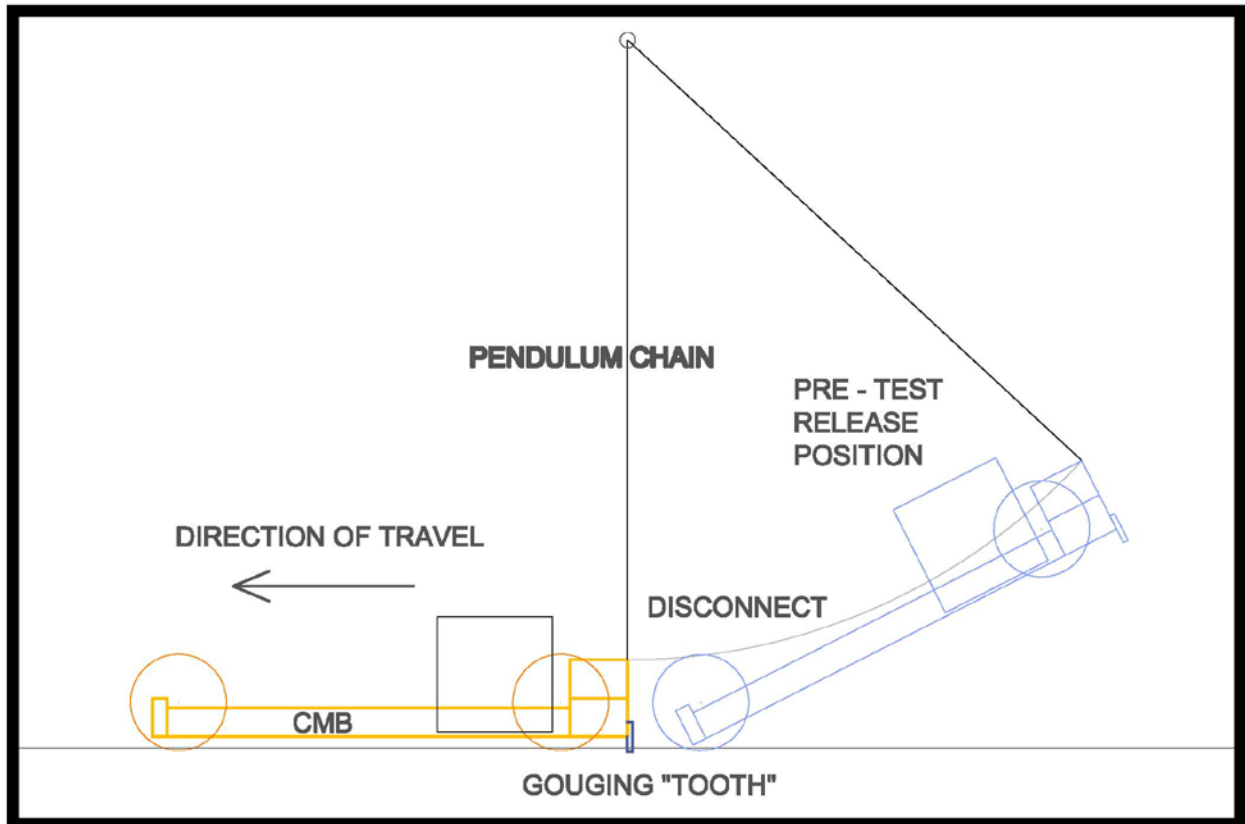


Figure 2.3 Test vehicle setup of previous testing done [Warner 2008]

gouge to get the energy that was absorbed by creating the gouge. The following equations show this technique:

$$F_{avg} = A_{avg} \times 5223 \text{ psi} \quad (2.9)$$

$$E_{gouge} = F_{avg} L_{gouge} \quad (2.10)$$

where F_{avg} = average force over the entire length of the gouge, A_{avg} = average cross-sectional area of the gouge, E_{gouge} = energy of the gouge, and L_{gouge} = the length of the gouge. While this testing provided the first basis for gouge energy calculation, suggestions for further research were proposed by the authors. Asphalt surface temperature and gouging velocity were some of the aspects of the testing that could be improved upon to provide greater depth in the research. The current research also attempts to quantify instantaneous gouge areas with specific forces, whereas the previous testing only quantified the average area and average force over the entire gouge.

2.5 Roadway Surfaces

A large factor in the reconstruction of roadway gouges is the roadway surface itself. The research put forth did not attempt to quantify gouge forces based on changing roadway surface or paving techniques. However, there are different techniques used to form roadways and some background should be provided on these different techniques. While this list of roadway types is not an exhaustive record, it does reference the most common types of roadways. Information from this section was taken from the WAPA and WSDOT websites [WAPA, WSDOT].

2.5.1 Rigid Pavements

Rigid pavements are roadways that are paved with concrete or similar material. These roadways are rigid because of the stiff nature of the concrete material that is used. These roadways surfaces have many advantages because of the strength and longevity of the materials involved. However, because of the stiff nature of the material, creating and testing gouges on a rigid pavement is difficult and not as common as gouges on other types of roadways. For this

reason, this type of roadway was not considered during the current research. Figure 2.4 shows an example of a concrete roadway surface.

2.5.2 Cold Mix Asphalt Pavements

Cold mix asphalt pavements are materials that are typically between 0 degrees Fahrenheit (0° F) and 100° F when they are laid down. Cold mix asphalt consists of similar materials to hot mix asphalt (which is discussed later), but some chemicals and material are added so that the temperatures can be the same as the ambient temperature. Cold mix asphalts are typically used as a patch or repair on existing asphalt roadways. They are not used as the initial or new roadways



Figure 2.4 Example of a concrete roadway surface [FHWA]

surface. Because it is not a complete resurfacing solution, the cold mix patches tend to create uneven surfaces where the original surface meets with the patch work or fill. Cold mix patching is typically a short term solution to damaged roadways. Testing on cold mix asphalt roadways was not included as part of this research. Figure 2.5 shows cold mix asphalt being used as a roadway patching material.

2.5.3 Chip Seal Roadway Surfaces

A chip sealed roadway surface is a technique used to repair an existing roadway and extend its life before the roadway needs to be completely replaced. This techniques differs from the others in that the materials are not premixed, but are joined together on the existing roadway



Figure 2.5 Example of cold mix asphalt patching [Layfayette]

surface to be repaired. Liquid asphalt is sprayed onto the surface and then a layer of gravel is dumped over the asphalt. This gravel layer is then compacted into the liquid layer to bind them together. Excess gravel is then removed. The roadway now has a new layer on it that is typically very rough. This surface helps reduce glare and improves the skid resistance during wet weather. This type of roadway surface was not included as part of this research. Figure 2.6 shows a recently completed chip sealed roadway surface.

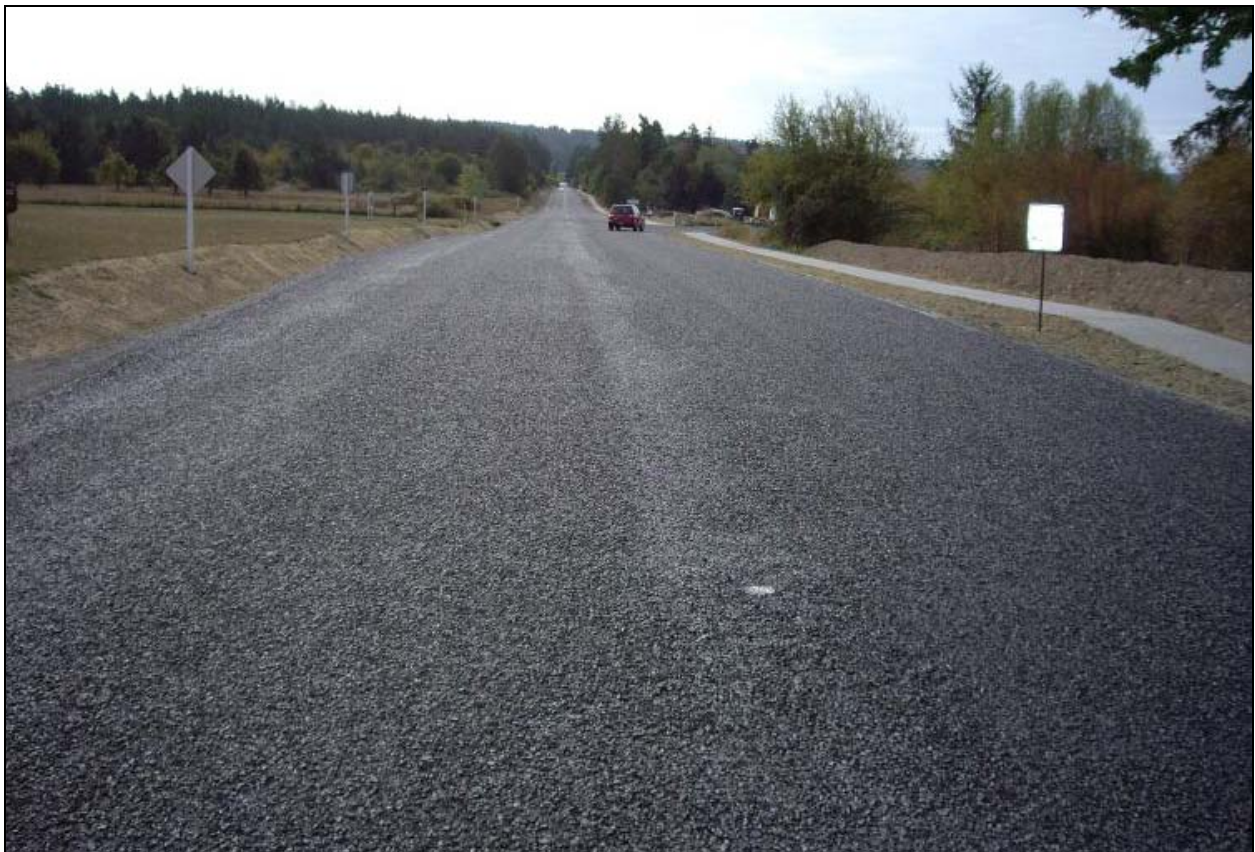


Figure 2.6 Example of newly paved chip seal [San Juan County News]

2.5.4 Hot Mix Asphalt

Hot mix asphalt (HMA) is the most common type of asphalt roadway surface. The binding agents and the aggregates are pre-mixed at a plant and then delivered to the paving site

at temperature (usually between 250° F and 350° F). This type of asphalt is typically laid as continuous strips of roadway and used for new surfaces. There are different mixtures and types of HMAs. Details on the different types will not be examined here, but can be readily found in other literature. Because of its commonality, this is the type of roadway surface that was used for the gouge tests. It also produces the most homogeneous surface and is easily penetrated making research and testing easier on the test equipment. Figure 2.7 shows an example of an HMA roadway surface.



Figure 2.7 Example of HMA roadway surface

3 TEST METHOD

This section outlines the methods, equipment, procedures, and conditions used during this research. All of the equipment and facilities used were owned and/or donated by Collision Safety Engineering, L.C. and Delta V Technology, Inc. in Orem, Utah, and Asphalt Zipper in American Fork, Utah.

3.1 Test Vehicle Set-up

To perform the testing on the asphalt, a utility van was ballasted and fitted with a hydraulic ram gouging mechanism, as shown in Figure 3.1. The test vehicle was also equipped with a power supply that powered the hydraulic ram. An A-frame swing arm system was constructed and attached to the frame of the vehicle. The A-frame system allowed the gouging tooth to be retracted up and out of the way during transport of the vehicle to the testing locations. This also allowed the vehicle to reach the desired speed and position during the test without causing or creating any undesired roadway damage. Once the desired speeds were reached, the swing arm enabled the gouging tooth to be deployed into the roadway surface. When the test run was complete, the gouging tooth could then be retracted out of the roadway surface and the vehicle could be moved again without further damage to the road. Controls for the hydraulic ram system were located next to the driver's seat so that the entire test could be performed by a single driver. This eliminated the need to coordinate speeds and deployment among multiple individuals providing more consistent speeds and tooth deployment. The ram itself was attached

to the end of the A-frame close to the tooth location so that the vertical force induced by the ram was transferred as directly as possible to the gouging tooth.

The tooth was made of hardened steel with a tungsten carbide tip. It is a tooth that is used commonly in the mining industry and this particular tooth was designed for tearing out asphalt roadways. Figure 3.1 show a profile picture of the tooth used to show the tooth's geometry.



Figure 3.1 Picture of gouge tooth used during testing

This tooth was changed out after each test. Running multiple tests on a single tooth produced too much wear on the tooth, which made for inconsistent data in the subsequent test. This made it necessary to use a new tooth for each test. The horizontal loads of the gouging force were transmitted to the frame of the van through the A-arm.

A concrete ballast block was mounted in the rear of the test vehicle to provide a larger mass to increase the force between the tooth and the roadway. The deceleration of the van was then measured using a Vericom 3000 computer. The Vericom has a built in spring-mass accelerometer and handles all of the self zeroing, recording, and storing of data. The Vericom accelerometer was mounted in the front of the vehicle near the driver so that, again, all functions of the test could be performed by a single individual. Figure 3.2 shows the profile view of the gouging setup.

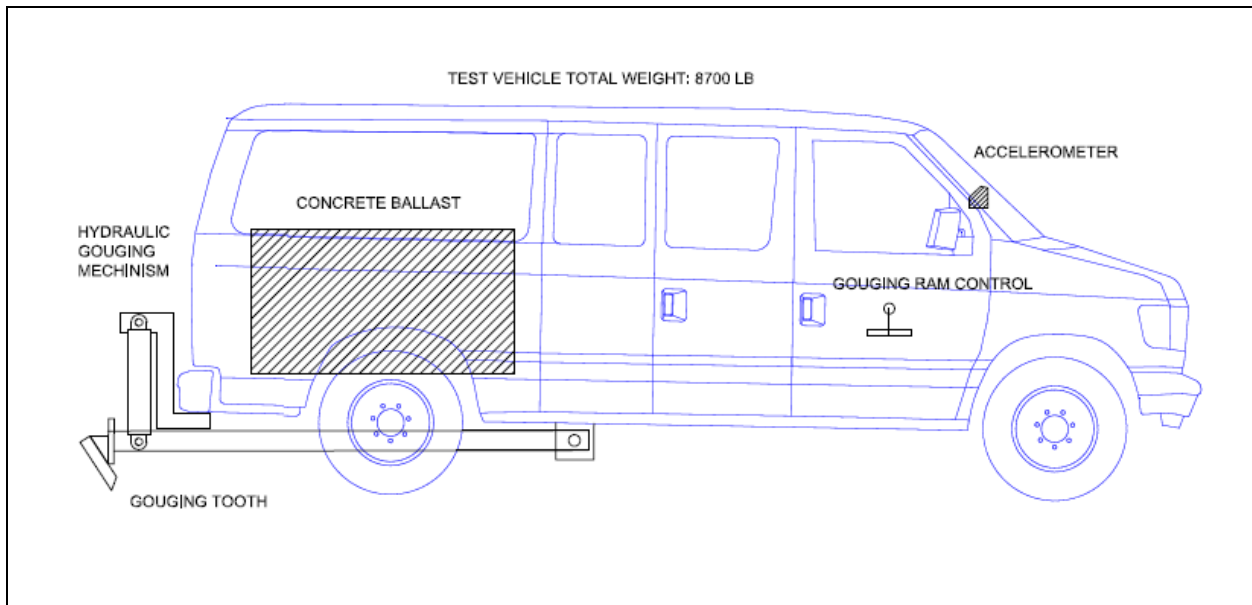


Figure 3.2 Gouge test vehicle configuration

The total weight of the test vehicle with driver was 8700 lbs. The total weight was measured on an industrial scale with a resolution of +/- 10 lbs. The same weight was used in all tests to make the necessary force calculations from the accelerometer data.

3.2 Test Conditions – Vehicle

For each test, the same protocol was employed relating to operation of the test vehicle. Parameters such as tire pressure and total mass were held constant and the same driver performed all of the tests. All tests were performed with the automatic transmission in the drive position for the duration of the test. Upon selection of the sample location and preparation of the vehicle, the operator would initiate the accelerometer and bring the vehicle to speed. At the desired speed and location, the operator removed his foot from the accelerator pedal allowing the vehicle to coast under its own momentum and deployed the gouging mechanism using the controls that were mounted next to the driver's seat. This activated the hydraulic ram which deployed the tooth vertically downward into the sample asphalt.

During the downward motion of the gouging tooth, the horizontal force caused by the removal of asphalt from the roadway and the subsequent deceleration of the test vehicle increased due to the increasing depth of the resulting gouge and increasing energy required to disrupt the road surface. Test vehicle motion was brought to a halt by gouge forces alone that were created by the tooth (again the brakes were not used at any time during the testing and the transmission was left in the Drive position and allowed to coast under its own momentum). Forces due to rolling resistance, wind resistance, and engine resistance were ignored because of their very small size in relation to the gouge forces. Once the vehicle came to a complete stop, the accelerometer was switched off to stop recording data and the tooth was removed from the roadway by raising the ram back up to its initial position. At this point, the acceleration was recorded and the sample gouge was measured and photographed.

3.3 Test Conditions – Roadway

Tests were chosen based on the characteristics that were to be tested. All tests were performed on a level section of roadway that was laid using hot mix asphalt. The exact composition of the HMA roadway was not determined. The temperature of the roadway was taken at the roadway surface. This is consistent with current roadway testing standards [SHRP] because measuring the temperature at any depth other than at the surface requires damaging it. Tests were performed while watching the weather to attempt to maximize temperature distribution. The tests were performed at different times of the day and on different days to achieve the temperature distribution desired. Testing early in the morning provided cooler temperatures, while the afternoons provided hotter temperatures. By varying the times the tests were completed, close to a 40° F temperature difference between coldest and hottest temperatures (95° F to 133° F) was realized.

All of the temperature related tests were performed at 15 mph. This was done in an attempt to minimize variation due to other factors that were not being tested in that set of tests. They were also performed on the same section of road so that roadway construction and type was also consistent between tests. Again, the temperature recorded was the surface temperature of the roadway at the location at which the test was being performed.

The higher speed test was performed at 25 mph. This was an increase of 10 mph over the previous set of tests. By increasing the speed 10 mph from 15 to 25, the amount of energy that would be dissipated by the gouge was more than doubled. To keep the high speed test consistent with the lower speed tests, it was performed at the same location. It was also performed at a temperature that was as close as possible to the lower temperature of the previous tests. Table 3.1 shows a summary of the test conditions for each test performed.

Table 3.1 Summary of Test Conditions for Each Test

Test	Speed (mph)	Temperature (F)	Kinetic Energy Absorbed (ft-lb)
1	15	95	65385
2	15	95	65385
3	15	133	65385
4	25	104	181625

The energy calculated in the above table is the same for all three 15 mph tests because the same vehicle was used with the same weight, the same speed was used each time and the vehicle was brought to a complete stop for each test. This meant that all the kinetic energy at the initiation of the gouge was completely transferred to the roadway in the form of gouge energy.

More than four tests were performed at these parameters. However, due to circumstances that are not fully understood, not all tests could be used for data analysis and conclusions for one reason or another. Some tests never penetrated the roadway surface and wore down the tooth. This could have been due to previous use of the gouge tooth or non-homogenous properties of the tooth or the roadway. Other tests did produce results that at first appeared to be valid but upon performing the numerical integration, the physical distance measured did not match up with the data from the accelerometer. These tests were subsequently not used in the analysis. The four tests used were the only ones to produce a gouge and have the recorded data match up with the physically measured data, thus the analysis could be performed with greater certainty on the results.

3.4 Test Procedure

For each test, the sample area that was to be gouged was chosen. The hydraulic system and tooth were then checked and set to their initial positions. The accelerometer was initialized

while the vehicle was still at rest so that it could properly zero calibrate. The vehicle was then brought up to the desired test speed and at a given start location, the vehicle was allowed to coast and the hydraulic ram was activated deploying the tooth into the asphalt surface. The vehicle was allowed to come to rest using only the gouge forces to decelerate and the acceleration curve measured was recorded and saved. The gouge geometry was then measured at 1 foot increments and the data was analyzed and reported.

3.5 Measurement Method

After a gouge was made, a tape measure was laid out next to the gouge and taped to the ground to prevent it from moving. 0 feet was measured at the location the vehicle came to rest and the gouge was measured from there. In other words, if the gouge is reported as being 100 feet long, the 100 foot mark is where the gouge was initiated at speed and the distance counts down to 0 feet which is where the vehicle came to rest and the gouge ended. Figure 3.3 shows an example of the tape measure placed next to the gouge.

Once the distance marks were established next to the gouge, a contour gage was used to measure the profile of the gouge. This contour gage is a standard 6 inch gage that can be purchased at most hardware stores. Figure 3.4 shows the contour gage used in measuring the gouge profiles. The contour gage was then placed into the gouge at one foot increments. The profile was recorded by placing the gage onto the ground at the place which the profile was to be measured and a photograph was taken. The photograph recorded both the profile of the gouge and the foot mark of that profile location. Figure 3.5 shows one of the photographs taken. The gouge profile was taken at one foot increments. Every profile was then photographed. The photographs were then loaded into a CAD drawing program. This was done so that the

photographs could be scaled properly and then the profile could be traced. By creating an enclosed area around the gouge profile, an accurate measure of the area could automatically be calculated. Figure 3.6 shows the tracing of the same photograph shown in Figure 3.5.



Figure 3.3 Tape measure next to gouge



Figure 3.4 Contour gage used for profile measurements



Figure 3.5 Example of photograph used to record gouge profile

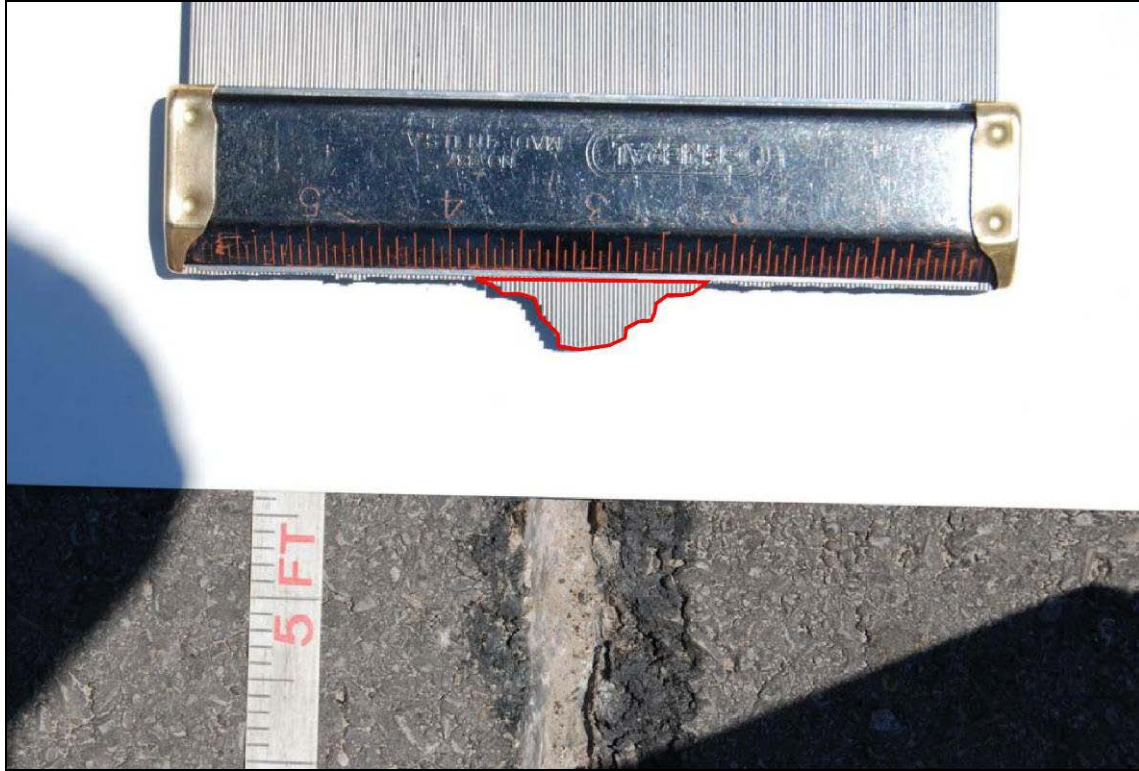


Figure 3.6 CAD drawing of gouge profile used for area measurement

Every photograph of every gouge profile was done this way to calculate the cross-sectional area of the gouge at the one foot increments. This data was collected for every gouge and then compared to the acceleration data that corresponded with it.

3.6 Accelerometer Data

The accelerometer used has a self-zeroing function that was performed at the beginning of every test. This is done while the test vehicle was at rest, before it was accelerated up to the test speed. The acceleration data was used to find the acceleration at every one foot increment so that it could be coordinated with the area data. This was done by integrating the accelerometer data twice to get distance. The acceleration at its distance calculated could then be synchronized with the cross-sectional area at the same distance. When an acceleration point did not match

perfectly with a one foot increment, a linear interpolation was used around that foot mark to obtain an acceleration value.

The way the testing was done coupled with the type of accelerometer used introduced some extra forces that needed to be filtered out before the data could be used. This was due to the fact that the hydraulic ram would actually lift the back of the van up a few inches when it was completely deployed. Because the accelerometer was a spring-mass system, the tilt introduced by the ram on the vehicle caused the accelerometer to read non-zero accelerations, even though the vehicle was at rest. This extra acceleration had to be removed in order to use the data. This step was relatively simple. A static test was done with the accelerometer recording data. The accelerometer was zero adjusted and then the hydraulic ram was deployed with the vehicle at rest. The induced acceleration was measured and recorded. For each of the dynamic tests performed, the acceleration that was taken in the static test was subtracted from the dynamic test data to produce the corrected acceleration trace which was then used for data analysis. Figure 3.7 shows a graph of two acceleration traces. One is the raw data from an example test and the other is the corrected data. There are a few key points to make about Figure 3.7. Notice that the two sets of data are exactly the same until the ram is deployed. This is where the acceleration begins to go negative, indicating that the vehicle is beginning to slow down. As the ram is deployed further into the roadway, the difference between the raw data and the corrected data becomes larger. Notice that at the end of the test, when the vehicle has come to a complete stop, there should be no acceleration, meaning, the acceleration trace should be at zero (which is where it started at the beginning of the test). The raw data however did not end at zero acceleration, but still had some negative acceleration. Again, this was due to the tilt in the vehicle that was induced by the deployed ram. The corrected data took into account the error caused by the tilt of

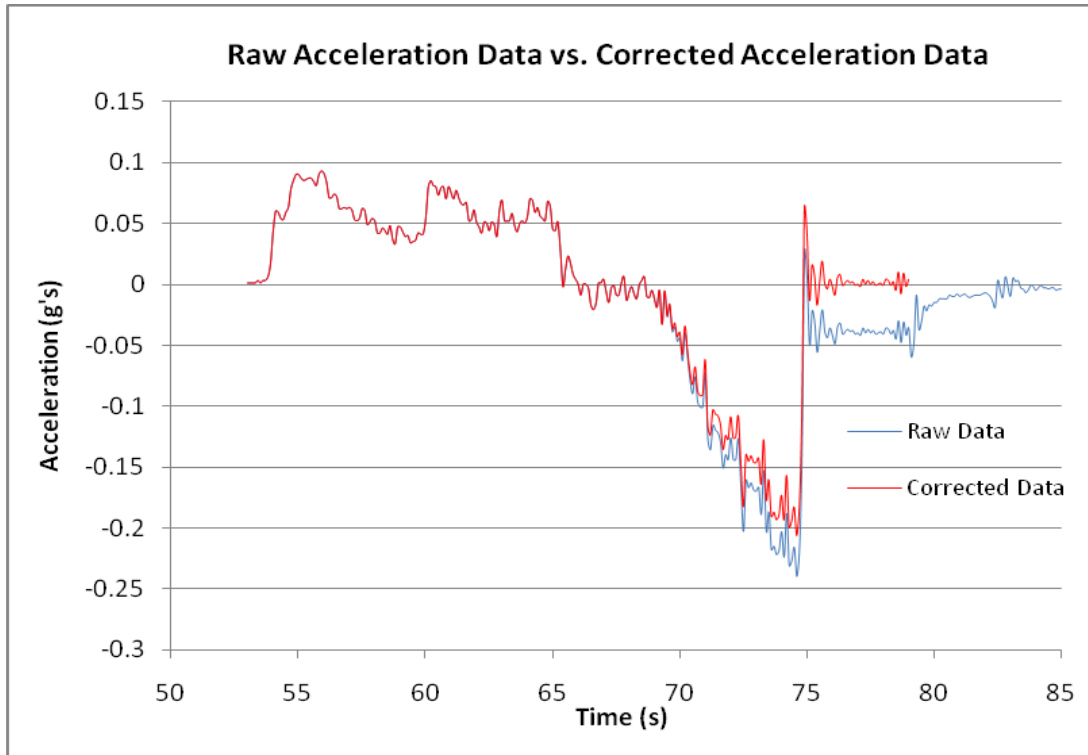


Figure 3.7 Example of raw accelerometer data vs. corrected accelerometer data

the vehicle and subtracted this error out of the original acceleration data. Notice the corrected data does end at zero acceleration. This procedure was employed in all four tests. All four resulted in zero acceleration when the vehicle came to a complete halt, even with the ram still deployed. With the corrected acceleration data, the velocity, distance, and force were calculated by using numerical integration. The corrected acceleration was integrated to get the velocity at that point and then integrated again to get the distance. This integration was checked to make sure that the distance of the gouge measured with a tape measure was the same that was obtained through the numerical integration. Once the data was verified to be ok, the force was calculated by multiplying the corrected acceleration by the weight of the vehicle. Every acceleration point now had a corresponding velocity, distance, and force. The data could then be coordinated with

the measured cross-sectional area measurement at every one foot increment which allowed for the comparisons made in the results section to be obtained.

4 RESULTS

The results of the testing were comparable to the previous testing done at lower speeds based on the average pressure along the gouge length [Warner M]. However, refinements in the test method allowed more detailed data to be collected and analyzed. Figure 4.1 shows an example of a gouge right after the completion of a run.



Figure 4.1 Post-test roadway gouge

The results are plotted comparing the cross-sectional area of the gouge at one foot intervals with the force measured at the same interval location. Figure 4.2 shows gouge force test results for a 15 mph test at a surface temperature of 95 degrees F.

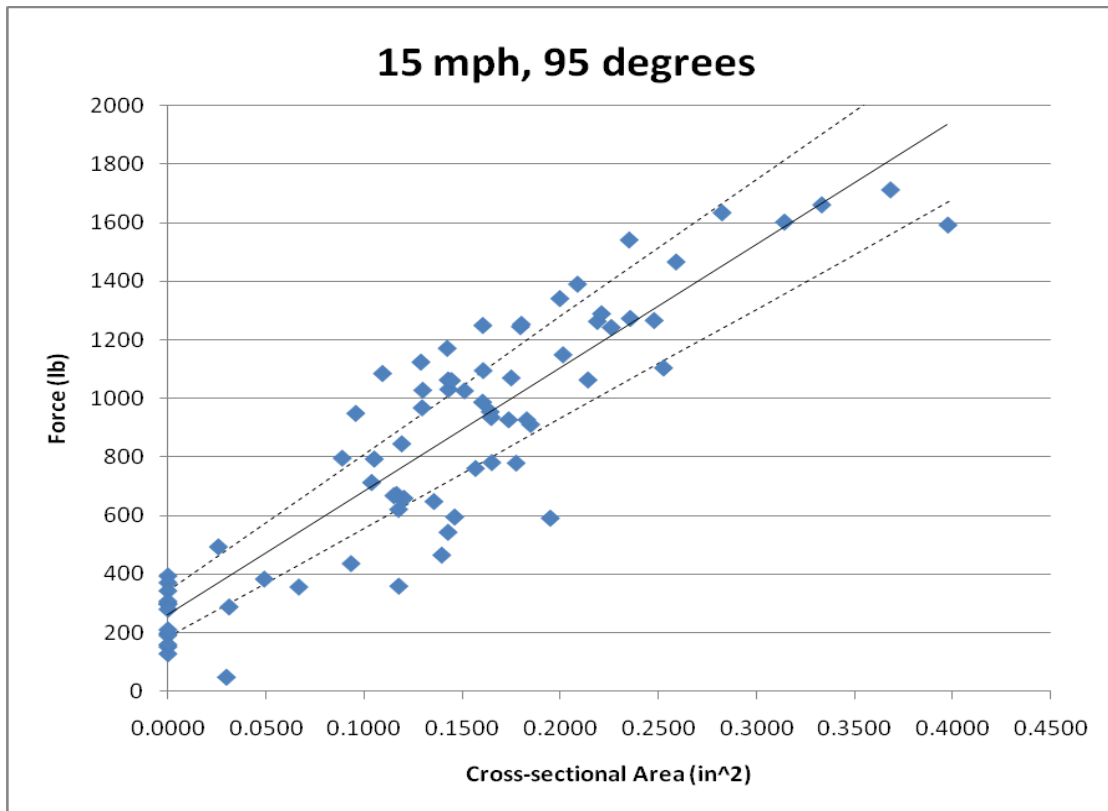


Figure 4.2 Asphalt gouge at 15 mph at 95° F surface temperature

By comparing the force with the cross-sectional area, a linear distribution is achieved. The line shown represents a linear best fit line. The equation for the line is

$$F = 4215.3A + 261.9. \tag{4.1}$$

A 95% confidence interval was also calculated and plotted around the line. Scraping the surface of the asphalt resulted in measurable force even though there was no measurable area removed from the roadway. This is what gives the equation a non-zero y intercept. The gouging done

while the vehicle was very close to rest (meaning at 1 or 2 mph) was not a true dynamic gouge. The accelerometer was only measuring the horizontal accelerations but at low speeds, the vertical forces became significant. There was no way to account for these forces and thus the points were discarded. Figure 4.3 shows the same test as in Figure 4.2 but with the low speed point included. These points were excluded when calculating the best fit line. They had a much larger cross-sectional area but did not increase the horizontal force. When the vehicle was at rest, the tooth was noticeably sinking into the asphalt because of the vertical weight on it. This is what a caused large area to be measured, but small horizontal forces.

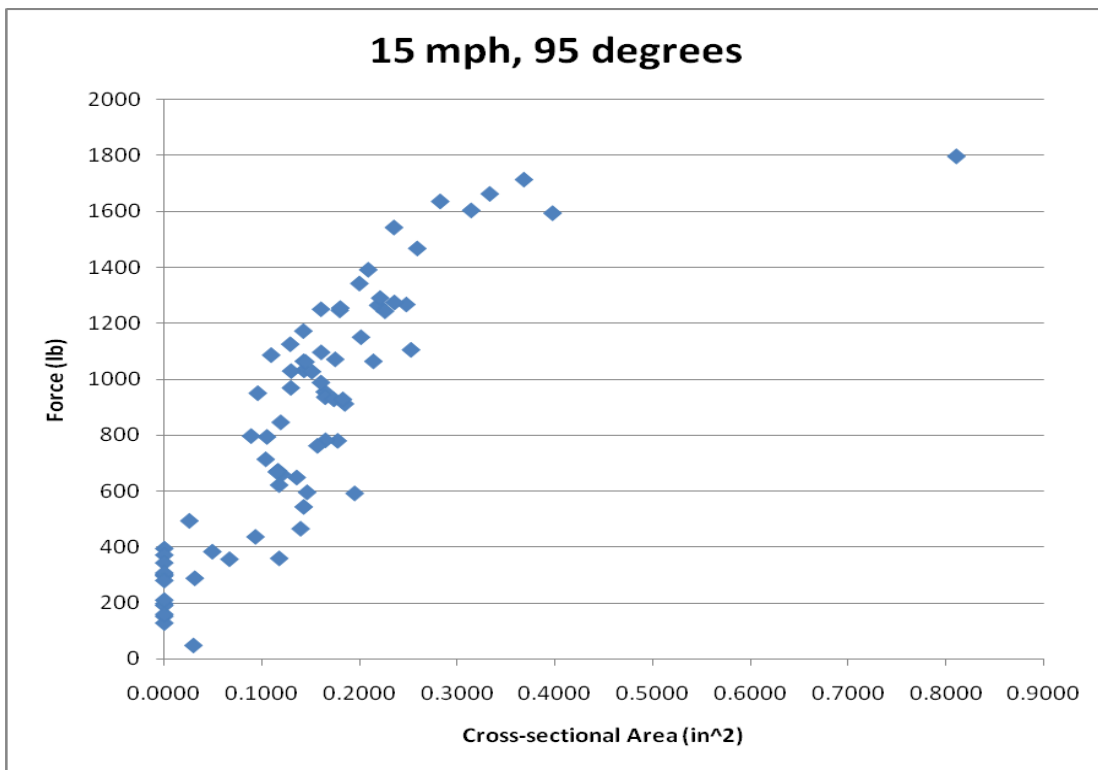


Figure 4.3 Asphalt gouge at 15 mph at 95° F showing all points

As can be seen in Figure 4.3, the low velocity point shown is clearly an outlier due to the small speed at which the test vehicle was traveling at this point. Again, this was because the

tooth was sinking into the roadway due to the vertical load being much greater than any horizontal load. Including this point would introduce results of static deformation into the dynamic testing.

A second test was performed with the same parameters to test the variation in data from one run to the next. This run yielded similar results and provided a best fit line of

$$F = 4054.4A + 217.4. \tag{4.2}$$

This shows that repeatability of the test is good and that variation in the roadway tested was low.

One of the main parameters to be tested was the effect of temperature on the asphalt that was being gouged. A test was conducted at the same location as the previous two tests, but was performed when the surface temperature was 133 degrees. Figure 4.4 shows the results of the higher temperature test.

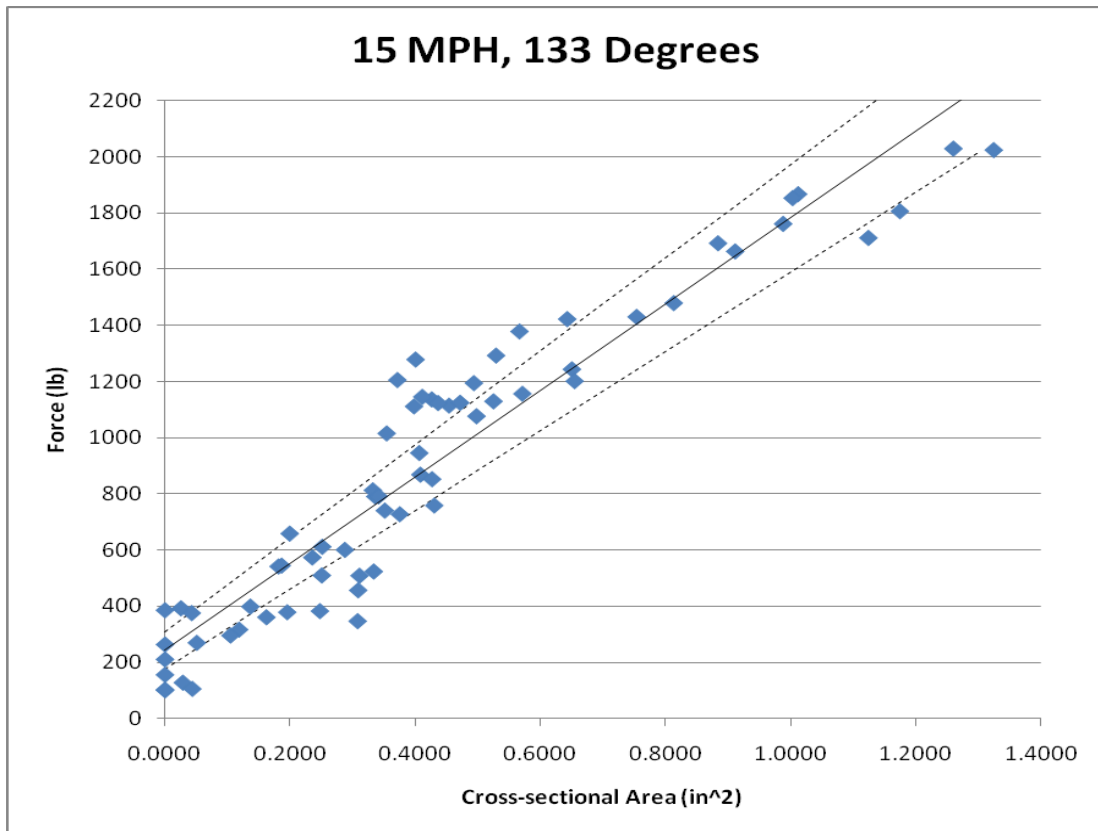


Figure 4.4 Asphalt gouge at 15 mph at 133° F

The results of this test were much different than the previous two. The linear best fit yielded an equation of

$$F = 1538.5A + 243.4. \quad (4.3)$$

While the intercept is very close to the other tests, the slope is less steep which indicates that a much larger area of asphalt is removed from the roadway with about the same amount of force as in the previous tests. For example, a force of 1500 lbs at 95° F would cause a gouge with a cross-sectional area of approximately 0.32 in², based on the linear fit. That same 1500 lbs force at 133° F would create a 0.82 in² cross-sectional area gouge. This shows that as the temperature of the asphalt increases, its ability to resist gouging decreases, or it becomes “softer”. For this particular roadway surface, the difference in temperature from 95° F to 133° F changed the slope of the linear fit line by a factor of approximately 2.5. This indicates that temperature is a significant factor in the determination of gouge force and energy.

A single test was also performed at 25 mph to see if there was any change based on the initial speed of the test. The temperature was chosen to be as close to 95° F as possible to attempt to reduce any temperature influence on the test. The resulting temperature for the test was 104° F. Figure 4.5 shows the results of that test.

There were several differences between this test and the previous tests. First, the gouge itself was much longer in distance as shown by the large increase in data points. Second, the intercept is much larger than the slower runs (500 compared to approximately 250). The intercept shows the force on the part of the asphalt that was being scraped, but was not producing any measurable gouge. This means the force on the asphalt was higher, but due to the speed of the gouging tooth moving across the surface, no measurable penetration into the asphalt was created. The third notable difference with this run was the slope of the best fit line. The equation

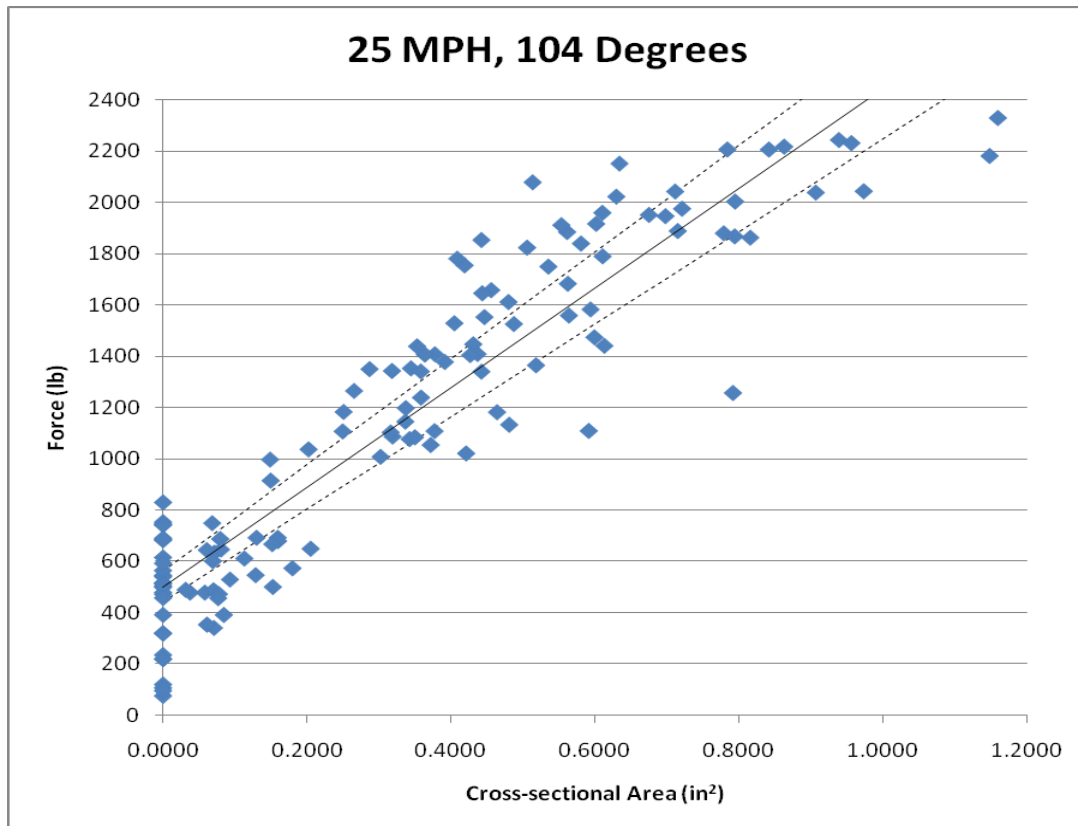


Figure 4.5 Asphalt gouge at 25 mph at 104° F

produced was

$$F = 1941.6A + 500.5. \tag{4.4}$$

The slope of the line was greater than the hot temperature test, but not as steep as the test done at a similar temperature, but at the lower speed. This would indicate that at higher speeds, the asphalt "flows" differently around the gouging tooth than it does at lower speeds. Table 4.1 shows a summary of the tests that were performed.

Table 4.1 Summary of Tests Performed

Test	Speed (mph)	Temperature (F)	Best Fit	Average Pressure (psi)
1	15	95	$F = 4215.3A + 261.9$	6000
2	15	95	$F = 4054.4A + 217.4$	5500
3	15	133	$F = 1538.5A + 243.4$	2400
4	25	104	$F = 1941.6A + 500.5$	3300

Despite some change in results based on speed, temperature appears to be a more significant factor in the determination of forces in asphalt gouging. An equation used in roadway construction relates the surface temperature of an asphalt roadway to its modulus [SHRP], which is given by

$$\text{Log}E = 6.464 - 0.000145 - T^{1.94824} \quad (4.5)$$

Where T is the surface temperature in degrees F and E is the modulus of the asphalt. Figure 4.6 shows the temperature and pressure relationship that was observed during the testing. The trend line shown is a Power fit to the data points collected.

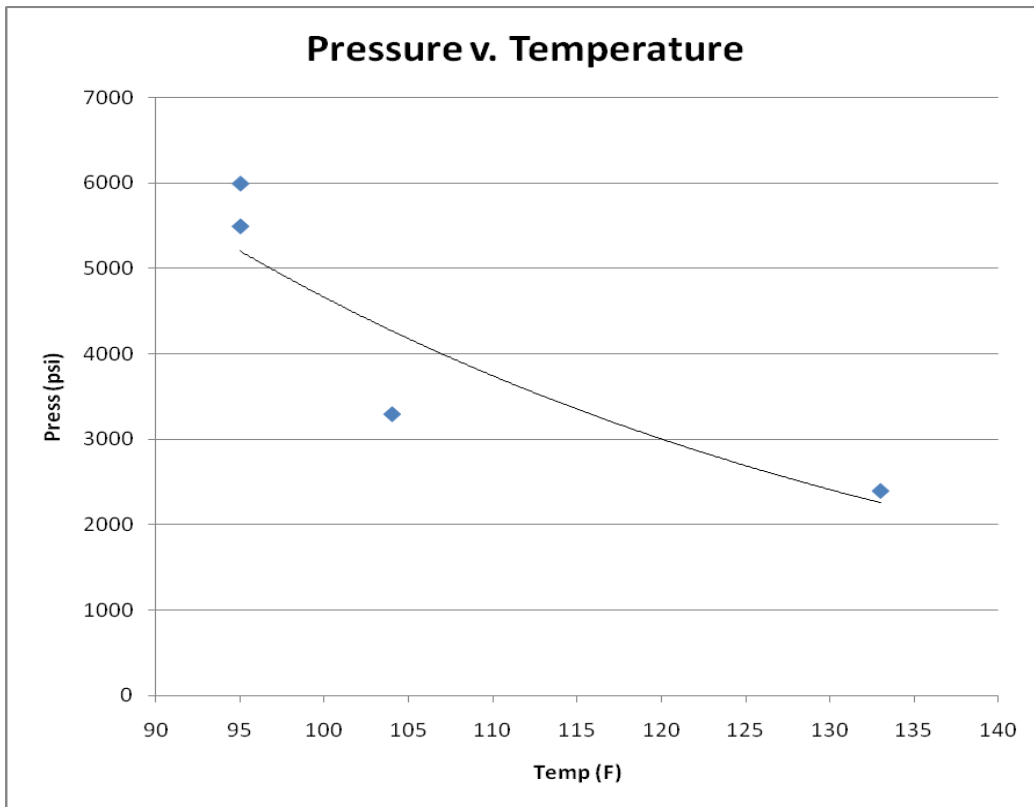


Figure 4.6 Pressure v. temperature of the tests completed

The modulus equation (4.5) was plotted in order to compare the general trend of the modulus of asphalt related to temperature with the pressure observed during testing. Figure 4.7 shows the modulus equation graphed from 90° F to 140° F. The pressure based analysis and results from this testing produce a curvature similar to that described by the sample modulus equation. This result is not unexpected because both are temperature based and the modulus of a sample should be proportionally related to the amount of force or pressure it takes to deform it. This outcome may lead to the ability to extrapolate beyond our results to temperatures outside of our testing range and would allow reasonable estimates where testing is not available, but such a hypothesis has not been confirmed.

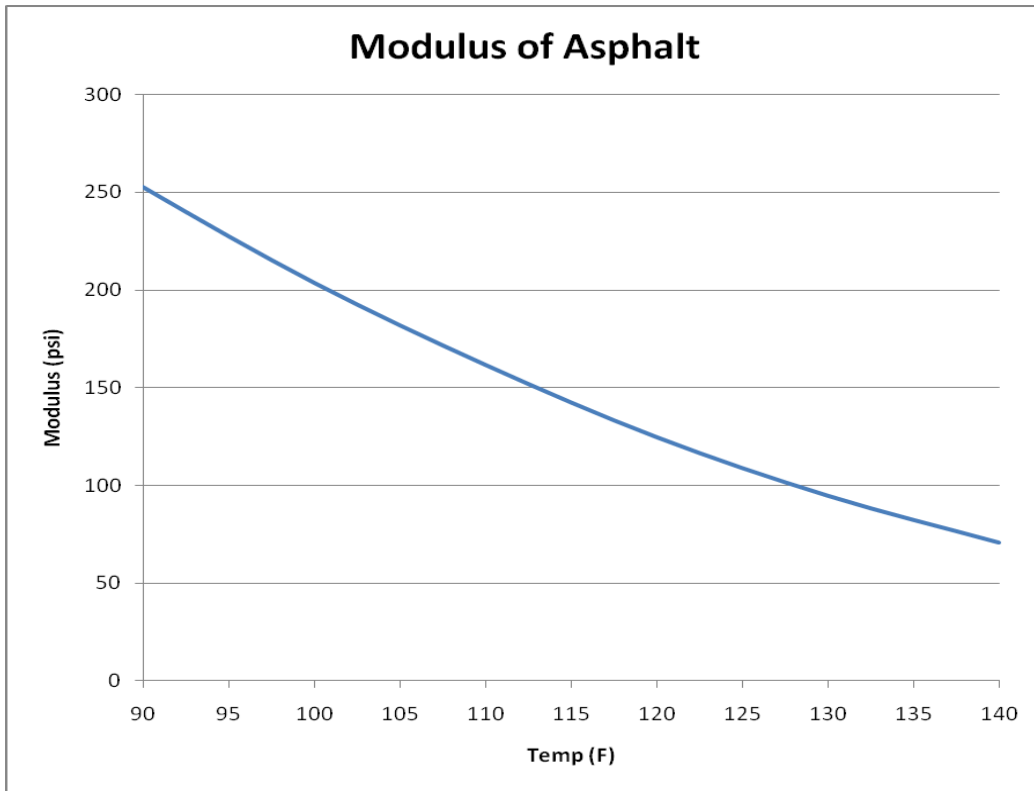


Figure 4.7 Modulus of asphalt

5 CONCLUSIONS

5.1 Test Method

The gouge technique used in this testing was an effective way to produce a repeatable roadway gouge. The test method was able to create the gouge and record the acceleration data and the cross-sectional area data. The method provided a way to correlate the cross-sectional area data with the acceleration data in the form of force. It was also effective in showing a trend in the data based on the surface temperature of the roadway surface to be tested.

5.2 Test Results

The testing provided results in the form of equations relating gouge cross-sectional area to the force that was required to produce that area. Table 5.1 reports the tests, the speed and temperature at which the test was performed, the equation relating the cross-sectional area with the force and the average pressure of the gouge over the entire length of the gouge. In the equation in Table 5.1, A is the cross-sectional area of the gouge and F is the resulting force.

Table 5.1 Summary of Test Results

Test	Speed (mph)	Temperature (F)	Best Fit	Average Pressure (psi)
1	15	95	$F = 4215.3A + 261.9$	6000
2	15	95	$F = 4054.4A + 217.4$	5500
3	15	133	$F = 1538.5A + 243.4$	2400
4	25	104	$F = 1941.6A + 500.5$	3300

5.3 Reconstruction Implication

Gouges in the asphalt are commonly considered to be an important part of vehicle accident reconstruction. Until now however, little data was available to make an energy estimate of the gouge energy. Now, using the cross-sectional area of a gouge at any location, a corresponding force can be estimated at that specific location using one of the equations shown in Table 5.1. Once a force is obtained for that location, it can be estimated over a chosen incremental distance to estimate the energy using

$$E_{gouge} = \Sigma(F_{gouge} d_{gouge}) \quad (5.1)$$

Where E_{gouge} = total gouge energy, F_{gouge} = force at the location measured, and d_{gouge} = distance between measurements of the gouge. The resulting energy estimate can then be used in the reconstruction of a crash and can provide greater detail into the steps of the crash being analyzed.

6 FUTURE RESEARCH

The testing done is a good beginning in a field of study that has yet to be researched to any great depth. This leads to the opportunity for further testing and discovery. The following is a list of recommendations for future work into roadway gouge energy:

- Number of samples – More tests are needed at the same parameters to further verify the results. The more tests that can be run, the greater the certainty can be on the results.
- Temperature – While the current research provided a large temperature gap of almost 40 degrees (95°F-133°F), greater temperature ranges need to be explored to verify the temperature relationship that was discovered. Temperatures down closer to freezing would be a reasonable goal to work with and would then provide data from 32° F up to 133° F, a range of over 100° F.
- Speed – The current research was only performed at two different speeds, with only a single test at the higher speed. In order to perform higher speed tests, a gouging tooth that is more wear resistant would need to be obtained. The teeth used during the current research only lasted for a single run. During higher speed tests, the tooth may not last for the whole run and thus skew the results.
- Gouge Geometry – The gouges used in the current tests had a limitation on depth and width because of the gouging tooth's geometry. Further testing into deep gouges and wide gouges would be highly beneficial because they are also common types of gouge geometries, especially when dealing with rollover accidents. The force required to make a

short, wide, deep gouge may not follow the same force trend that the long, skinny, shallows gouges did in the current set of testing.

- Vertical Force – Only the horizontal forces were measured because of the limitation of using an accelerometer to gather the data. A way of fitting a load cell or strain gage to the tooth would yield the vertical forces that are occurring as well and may reveal more details about the relationship between the vertical and horizontal forces going on which may explain why the largest forces were observed just before the test vehicle came to rest.
- Pavement Types – Only one type of roadway was tested (HMA) because it is the most common pavement type and therefore the results would apply to a large number of roadway gouges. However, other pavement types can be tested as well as gathering greater detail into the specific properties of the section of pavement tested.

REFERENCES

- Baker, J., Fricke, L., The Traffic-Accident Investigation Manual, Northwestern University Traffic Institute, Vol. 1 Ed. 9, Evanston, Illinois, ISBN 0-912642-06-8, 1986.
- Brach, R., Brach, M., Vehicle Accident Analysis and Reconstruction Methods, SAE International, Warrendale, Pennsylvania, ISBN 978-0768007763, 2005.
- Campbell, K., “Energy Basis for Collision Severity”, SAE Technical Paper 740565, Society of Automotive Engineers, Warrendale, Pennsylvania, 1974.
- Croteau, et al., “Determining closing speed in rear impact collisions with offset and override”, SAE Technical Paper 2001-01-1170, Society of Automotive Engineers, Warrendale, Pennsylvania, 2001.
- FHWA, *TechBrief: Daylighted Permeable Bases*, Federal Highway Administration, Accessed October 13, 2009, Available from <http://www.fhwa.dot.gov/pavement/concrete/pubs/hif09009/index.cfm>
- Fricke, L., Traffic Accident Reconstruction, Northwestern University Traffic Institute, Vol. 2 Ed. 1, Evanston, Illinois, ISBN 0-912642-06-8, 1990.
- Gillespie, T., Fundamentals of Vehicle Dynamics, Society of Automotive Engineers, Inc., Warrendale, Pennsylvania, 1992.
- Lafayette, *Asphalt & Concrete Repair*, City of Lafayette, Accessed October 13, 2009, Available from <http://www.lafayette.in.gov/egov/apps/services/index.egov?path=details&action=i&id=30>
- Limpert, R., Motor Vehicle Accident Reconstruction and Cause Analysis, The Michie Company, Charlottesville, Virginia, ISBN 0-87215-212-X, 1978.

Marine, et al., "Characteristics of On Road Rollovers", SAE Technical Paper 1999-01-0122, Society of Automotive Engineers, Warrendale, Pennsylvania, 1999.

Neptune, J., Flynn, J., "A Method for Determining Accident Specific Crush Stiffness Coefficients", SAE Technical Paper 940913, Society of Automotive Engineers, Warrendale, Pennsylvania, 1994.

Neptune, J., Flynn, J., "A Method for Determining Crush Stiffness Coefficients from Offset Frontal and Side Crash Tests", SAE Technical Paper 980024, Society of Automotive Engineers, Warrendale, Pennsylvania, 1998.

NHTSA, Traffic Safety Facts 2008 Data, National Highway Traffic Safety Administration, Accessed October 14, 2009, Available from <http://www-nrd.nhtsa.dot.gov/Pubs/811162.PDF>

Orlowski, K., et al., "Reconstruction of Rollover Collisions", SAE Technical Paper 890857, Society of Automotive Engineers, Warrendale, Pennsylvania, 1989.

PC Crash, PC Crash Manual Version 8.1.

San Juan County News, Fisherman Bay Road Reopens, Accessed October 13, 2009, Available from <http://www.sanjuanco.com/News/CountyNews.aspx?NewsItem=225>.

Sens, et al., "Perception/reaction time values for accident reconstruction", SAE Technical Paper 890732, Society of Automotive Engineers, Warrendale, Pennsylvania, 1989.

SHRP, *Strategic Highway Research Program: Procedure for Temperature Correction of Maximum Deflections*, SHRP-P-654, National Research Council, Washington D.C., 1993.

SMAC, SMAC User Manual, 1994.

Strother, C., Kent, R., Warner, C., "Estimating vehicle deformation energy for vehicles struck in the side", SAE Technical Paper 980215, Society of Automotive Engineers, Warrendale, Pennsylvania, 1998.

Strother, C., Woolley, R., James, M., Warner, C., "Crush Energy in Accident Reconstruction", SAE Technical Paper 860371, Society of Automotive Engineers, Warrendale, Pennsylvania, 1986.

Uchida, et al., "Effects of Hands-Free Phone Conversation on Visual Behavior: Dissociation of Binocular Gaze Point as an Index of Inattention", SAE Technical Paper 2005-01-0439, Society of Automotive Engineers, Warrendale, Pennsylvania, 2005.

Varat, et al. "The analysis and determination of tire-roadway frictional drag", SAE Technical Paper 2003-01-0887, Society of Automotive Engineers, Warrendale, Pennsylvania, 2003.

Vilardo, F., "Relative risk of alcohol involved crashes", SAE Technical Paper 870601, Society of Automotive Engineers, Warrendale, Pennsylvania, 1986.

Wallingford, et al., "Tire-Roadway Friction Coefficients on Concrete and Asphalt Surfaces Applicable for Accident Reconstruction", SAE Technical Paper 900103, Society of Automotive Engineers, Warrendale, Pennsylvania, 1990.

WAPA, *The WAPA Asphalt Pavement Guide*, Washington Asphalt Pavement Association, Accessed October 13, 2009, Available from http://www.asphaltwa.com/pavement_guide/pavement_guide.htm.

Warner, C., Allsop, D., Germane, G., "A repeated-Crash Test Technique for Assessment of Structural Impact Behavior", SAE Technical Paper 860208, Society of Automotive Engineers, Warrendale, Pennsylvania, 1986.

Warner, M., *Development of pole impact testing at multiple vehicle side location as applied to the Ford Taurus structural platform*, MS Thesis, Brigham Young University, 2004.

Warner, M., Warner, C., Crosby, C., "Roadway Asphalt Damage Force Analysis For Accident Reconstruction", SAE Technical Paper 2008-01-0173, Society of Automotive Engineers, Warrendale, Pennsylvania, 2008.

WSDOT, *Eastern Region Chip Seal*, Washington State Department of Transportation, Accessed October 14, 2009, Available from <http://www.wsdot.wa.gov/Regions/Eastern/ChipSeal/Default.htm>

APPENDIX A RAW TEST DATA

This is the raw data from one of the runs at 15 mph at 95° F. This is to show how the raw data looked and how it was used to calculate the force vs. cross-sectional area graphs.

Table A.1 Raw Test Data of 15mph Test at 95° F

Test 1	5/14/2009	12:05 PM	Time	Speed -	15 MPH	Temp-	95 F
Time	Accel	Accel	Accel	Speed	Speed	Distance	Force
Sec	G	Offset	Corrected	ft/s	MPH	Ft	lb
69.3	-0.033	0.00000	-0.03300	21.61	14.73	75.15	-287.1
69.4	-0.006	0.00063	-0.00537	21.55	14.69	72.99	-46.7
69.5	-0.027	0.00127	-0.02573	21.50	14.66	70.84	-223.9
69.6	-0.018	0.00190	-0.01610	21.43	14.61	68.69	-140.0
69.7	-0.039	0.00254	-0.03646	21.35	14.55	66.55	-317.2
69.8	-0.035	0.00317	-0.03183	21.24	14.48	64.42	-276.9
69.9	-0.047	0.00381	-0.04319	21.11	14.40	62.31	-375.8
70	-0.044	0.00444	-0.03956	20.98	14.31	60.20	-344.1
70.1	-0.063	0.00508	-0.05792	20.82	14.20	58.11	-503.9
70.2	-0.040	0.00571	-0.03429	20.68	14.10	56.04	-298.3
70.3	-0.060	0.00635	-0.05365	20.53	14.00	53.97	-466.8
70.4	-0.079	0.00698	-0.07202	20.33	13.86	51.93	-626.5
70.5	-0.090	0.00762	-0.08238	20.08	13.69	49.91	-716.7
70.6	-0.076	0.00825	-0.06775	19.84	13.53	47.91	-589.4
70.7	-0.097	0.00889	-0.08811	19.59	13.36	45.94	-766.6
70.8	-0.101	0.00952	-0.09148	19.30	13.16	44.00	-795.8
70.9	-0.101	0.01016	-0.09084	19.01	12.96	42.08	-790.3
71	-0.073	0.01079	-0.06221	18.76	12.79	40.19	-541.2
71.1	-0.128	0.01143	-0.11657	18.47	12.60	38.33	-1014.2
71.2	-0.136	0.01206	-0.12394	18.09	12.33	36.50	-1078.2
71.3	-0.116	0.01270	-0.10330	17.72	12.08	34.71	-898.7
71.4	-0.120	0.01333	-0.10667	17.38	11.85	32.96	-928.0
71.5	-0.122	0.01397	-0.10803	17.04	11.62	31.24	-939.9
71.6	-0.130	0.01460	-0.11540	16.68	11.37	29.55	-1004.0
71.7	-0.151	0.01524	-0.13576	16.27	11.10	27.90	-1181.1
71.8	-0.140	0.01587	-0.12413	15.85	10.81	26.30	-1079.9
71.9	-0.144	0.01651	-0.12749	15.45	10.53	24.73	-1109.2

Table A.1 Continued

Time	Accel	Accel	Accel	Speed	Speed	Distance	Force
72	-0.126	0.01714	-0.10886	15.07	10.27	23.21	-947.1
72.1	-0.144	0.01778	-0.12622	14.69	10.02	21.72	-1098.1
72.2	-0.144	0.01841	-0.12559	14.29	9.74	20.27	-1092.6
72.3	-0.127	0.01905	-0.10795	13.91	9.48	18.86	-939.2
72.4	-0.166	0.01968	-0.14632	13.50	9.20	17.49	-1273.0
72.5	-0.203	0.02032	-0.18268	12.97	8.84	16.17	-1589.3
72.6	-0.161	0.02095	-0.14005	12.45	8.49	14.89	-1218.4
72.7	-0.167	0.02159	-0.14541	11.99	8.18	13.67	-1265.1
72.8	-0.163	0.02222	-0.14078	11.53	7.86	12.50	-1224.8
72.9	-0.169	0.02286	-0.14614	11.07	7.55	11.37	-1271.4
73	-0.170	0.02349	-0.14651	10.60	7.23	10.28	-1274.6
73.1	-0.167	0.02413	-0.14287	10.13	6.91	9.25	-1243.0
73.2	-0.189	0.02476	-0.16424	9.64	6.57	8.26	-1428.9
73.3	-0.153	0.02540	-0.12760	9.17	6.25	7.32	-1110.1
73.4	-0.203	0.02603	-0.17697	8.68	5.92	6.43	-1539.6
73.5	-0.187	0.02667	-0.16033	8.13	5.55	5.59	-1394.9
73.6	-0.218	0.02730	-0.19070	7.57	5.16	4.80	-1659.1
73.7	-0.215	0.02794	-0.18706	6.96	4.75	4.07	-1627.5
73.8	-0.222	0.02857	-0.19343	6.35	4.33	3.41	-1682.8
73.9	-0.219	0.02921	-0.18979	5.73	3.91	2.80	-1651.2
74	-0.203	0.02984	-0.17316	5.15	3.51	2.26	-1506.5
74.1	-0.224	0.03048	-0.19352	4.56	3.11	1.78	-1683.7
74.2	-0.188	0.03111	-0.15689	3.99	2.72	1.35	-1364.9
74.3	-0.231	0.03175	-0.19925	3.42	2.33	0.98	-1733.5
74.4	-0.227	0.03238	-0.19462	2.78	1.90	0.67	-1693.2
74.5	-0.216	0.03302	-0.18298	2.18	1.48	0.42	-1592.0
74.6	-0.240	0.03365	-0.20635	1.55	1.06	0.23	-1795.2
74.7	-0.219	0.03429	-0.18471	0.92	0.63	0.11	-1607.0
74.8	-0.142	0.03492	-0.10708	0.45	0.31	0.04	-931.6
74.9	0.027	0.03556	0.06256	0.38	0.26	0.00	544.2

The force at one foot intervals was then calculated and compared to the cross-sectional area at the same one foot increments. The next set of data shows the results.

Table A.2 Cross-section Area and Force of 15mph Test at 95° F

Ft	Area (in²)	Force	Pressure
0	0.8107	1795	2214
1	0.3681	1712	4651
2	0.3141	1602	5100
3	0.3331	1661	4986
4	0.2823	1634	5788
5	0.3974	1592	4006
6	0.2589	1466	5662
7	0.2188	1263	5772
8	0.1997	1341	6715
9	0.2209	1289	5835
10	0.2477	1266	5111
11	0.2355	1273	5406
12	0.1796	1245	6932
13	0.2259	1242	5498
14	0.1801	1253	6957
15	0.1604	1249	7787
16	0.2350	1541	6557
17	0.2087	1390	6660
18	0.2013	1149	5708
19	0.1642	954	5810
20	0.2140	1063	4967
21	0.1606	1095	6818
22	0.1749	1070	6118
23	0.1295	968	7475
24	0.1430	1031	7210
25	0.2525	1104	4372
26	0.1093	1085	9927
27	0.1289	1124	8720
28	0.1423	1171	8229
29	0.1428	1063	7444
30	0.1603	987	6157
31	0.0957	949	9916
32	0.1647	935	5677
33	0.1736	927	5340
34	0.1848	911	4930
35	0.1828	927	5071
36	0.1298	1028	7920
37	0.1445	1061	7343

Table A.2 Continued

Ft	Area (in²)	Force	Pressure
38	0.1511	1026	6790
39	0.1191	845	7095
40	0.1948	591	3034
41	0.1355	648	4782
42	0.1774	779	4391
43	0.1051	793	7545
44	0.0888	796	8964
45	0.1650	781	4733
46	0.1567	761	4856
47	0.1165	672	5768
48	0.1461	595	4073
49	0.1203	659	5478
50	0.1038	713	6869
51	0.1151	668	5804
52	0.1175	621	5285
53	0.1427	543	3805
54	0.1395	465	3333
55	0.0491	383	7800
56	0.0000	301	N/A
57	0.0000	394	N/A
58	0.0257	493	19183
59	0.0933	436	4673
60	0.1176	359	3053
61	0.0667	356	5337
62	0.0000	371	N/A
63	0.0000	343	N/A
64	0.0000	297	N/A
65	0.0312	288	9231
66	0.0000	307	N/A
67	0.0000	280	N/A
68	0.0000	197	N/A
69	0.0000	152	N/A
70	0.0000	191	N/A
71	0.0000	210	N/A
72	0.0000	128	N/A
73	0.0298	48	1611
74	0.0000	159	N/A

APPENDIX B PHOTOGRAPHS





Photos showing 10 feet of gouge profiles as an example.











